

# TIME-VARYING COMPONENT OF THE SOLAR MERIDIONAL FLOW

Laurent Gizon<sup>1</sup> and Matthias Rempel<sup>2</sup>

<sup>1</sup>Max-Planck-Institut für Sonnensystemforschung, 37191 Katlenburg-Lindau, Germany

<sup>2</sup>High Altitude Observatory, NCAR, Boulder, CO 80307, USA

## ABSTRACT

We present helioseismic observations of the solar-cycle variation of flows near the solar surface and at a depth of about 60 Mm, in the latitude range  $\pm 45^\circ$ . The time-varying components of the meridional flow at these two depths have opposite sign, while the time-varying components of the zonal flow are in phase. We investigate a theoretical model based on a flux-transport dynamo combined with a geostrophic flow caused by increased radiative loss in the active region belt. The model and the data are in qualitative agreement, although the amplitude of the solar-cycle variation of the meridional flow at 60 Mm appears to be underestimated by the model.

## 1. OBSERVATIONS

For the near-surface layers, we used series of MDI full-disk Doppler images covering the period 1996-2002 and f-mode time-distance helioseismology [1] to obtain every 12 hour a  $120^\circ \times 120^\circ$  map of the horizontal divergence of the flow field 1 Mm below the photosphere. The flow  $\mathbf{v} = (v_x, v_y)$ , where  $x$  is prograde and  $y$  is northward, is obtained by measuring the advection of the supergranulation pattern according to the method of Gizon, Duvall & Schou [2]. This flow is likely to be an average over the supergranulation layer, which has been estimated to reach depths greater than 10 Mm [3]. Figure 1 is a plot of  $v_x(\lambda)$  and  $v_y(\lambda)$  for each full-disk MDI run as a function of latitude in the range  $|\lambda| < 50^\circ$ . To reduce noise, the north-south symmetric component of  $v_x$  and the antisymmetric component of  $v_y$  are extracted. Over the period 1996-2002,  $v_x$  varies by  $12 \text{ m s}^{-1}$  peak-to-peak at the equator (Fig. 1a). The Meridional flow is poleward with a mean amplitude of  $10 \text{ m s}^{-1}$  at latitude  $20^\circ$  (Fig. 1b). The peak-to-peak variation of the meridional flow is  $7 \text{ m s}^{-1}$  at  $\lambda = 30^\circ$ , i.e. a significant fraction of the time-averaged value. We estimate that the standard deviation of the noise at a particular latitude ( $5^\circ$  bin) for any given year is less than  $1 \text{ m s}^{-1}$ . The systematic errors that depend on position on the solar disk have been measured to be very low (less than  $5 \text{ m s}^{-1}$  over the whole region of analysis).

In order to probe deeper layers into the solar convec-

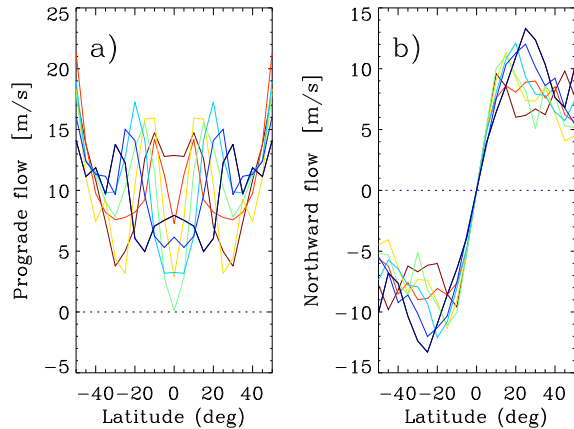


Figure 1. (a) Rotational velocity,  $v_x$ , and (b) meridional flow,  $v_y$ , near the solar surface as a function of latitude,  $\lambda$ . Each MDI dynamics run is plotted with a different color from blue in 1996 to red in 2002. The rotational velocity is given with respect to the rotational velocity of the small magnetic features [4].

tion zone, we used acoustic waves and time-distance helioseismology. Travel times were measured by cross-correlation of the Doppler oscillation signal recorded during the MDI structure program according to the procedure described by Giles [5]. Using a mean travel distance of  $17^\circ$  enables us to probe layers about 60 Mm below the surface. The full details of this analysis can be found in Beck, Gizon & Duvall [6]. In order to convert travel time shifts into flows in units of  $\text{m s}^{-1}$ , we use a simple calibration based on the observation by Howe et al. [7] (global-mode helioseismology) that the amplitude of the time-varying component of the zonal flow is nearly independent of depth. We choose the near-surface zonal flow measurements of the above paragraph as a reference.

In order to quantify the solar-cycle dependence of the flows, we extract the eleven-year periodic component from the data. At each latitude  $\lambda$  and for each depth, we fit a function of the form

$$\tilde{v}_i(\lambda, t) = \bar{v}_i(\lambda) + v'_i(\lambda) \cos \left[ \frac{2\pi t}{11 \text{ yr}} + \phi_i(\lambda) \right] \quad (1)$$

to the observed velocity  $v_i(\lambda, t)$ , where the index  $i$  refers

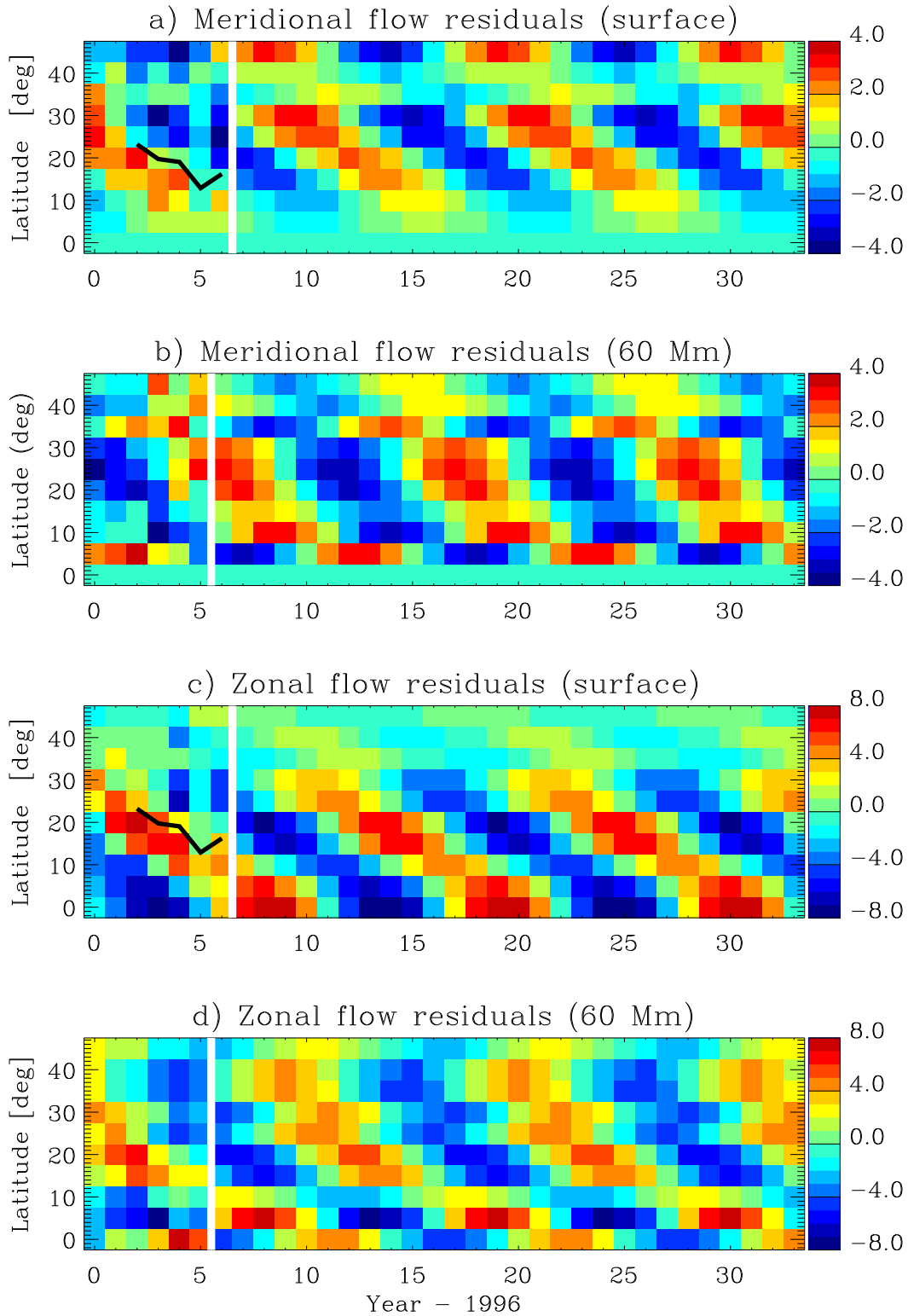


Figure 2. Eleven-year periodic component of the meridional and zonal flows. The color bar is in units of  $\text{m s}^{-1}$ . A positive value indicates a poleward (resp. prograde) meridional (resp. zonal) residual flow. The observations,  $v_i - \bar{v}_i$ , cover the first six years, while the purely sinusoidal component,  $\tilde{v}_i - \bar{v}_i$ , is extrapolated in time (beyond the vertical white line). The black curves indicate the mean latitude of magnetic activity.

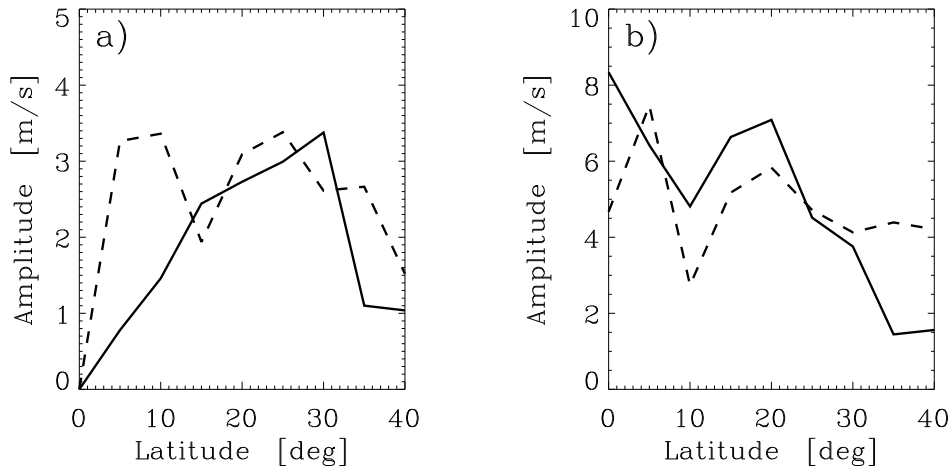


Figure 3. Amplitude,  $v'_i$ , of the eleven-year periodic component of the meridional (a) and zonal (b) flows. The near-surface values (solid lines) are absolute measurements. The calibration of the observations at 60 Mm depth (dashed lines) follows the assumption that the amplitude of the zonal torsional oscillation (panel b) is independent of depth over the latitude range  $|\lambda| < 45^\circ$ .

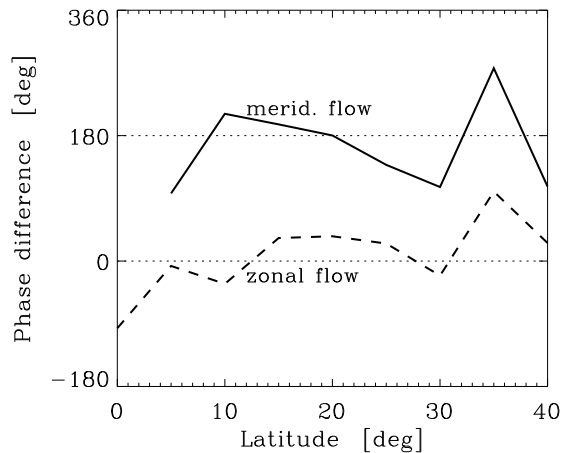


Figure 4. Phase difference,  $\Delta\phi = \phi(\text{deep}) - \phi(\text{surface})$ , between the eleven-year periodic components of the flows measured at a depth of 60 Mm and near the surface. The solid line is for the meridional flow and the dashed line is for the zonal flow.

to either the  $x$  or the  $y$  component of the flow. The long-term average is given by  $\bar{v}_i$ , while the amplitude and the phase of the time-varying component are denoted by  $v'_i$  and  $\phi_i$  respectively. It is somewhat arbitrary to presume that the variation of the flow with time is sinusoidal, although it appears to provide a reasonable description of the data.

The eleven-year periodic components of the meridional and zonal flows are shown in Figure 2. The torsional oscillation pattern is clearly seen at both depths with an

amplitude and a phase comparable to previous measurements [e.g. 7]. The meridional flow also contains a significant eleven-year periodic component. Near the solar surface, the residuals indicate the presence of a north-south inflow toward the mean latitude of activity [e.g. 8], while the data are consistent with a horizontal outflow from the mean latitude of activity deeper into the convection zone [e.g. 9, 6].

Figure 3 gives the amplitudes of the time-varying components of the flows,  $v'_i$ . Given the velocity calibration described above, the amplitude of the time-varying meridional flow,  $v'_y$ , is found to be approximately independent of depth ( $v'_y \simeq 3 \text{ m s}^{-1}$  at  $20^\circ$  latitude). The evidence that the time-varying components of the meridional flow near the surface and deeper in the interior are anti-correlated is given in Figure 4, which shows the difference in  $\phi_y$  at the two depths. On the contrary, there is no significant phase variation with depth for the zonal flow.

## 2. THEORETICAL MODEL

The model results presented here are based on a non-kinematic flux-transport dynamo model developed recently by Rempel [10, 11]. This model combines a differential rotation and meridional flow model [10] with a flux transport dynamo similar to the models of Dikpati & Charbonneau [12] and Dikpati & Gilman [13].

The differential rotation model utilizes a meanfield Reynolds-stress approach that parametrizes the turbulent angular momentum transport [14] leading to the observed equatorial acceleration. A meridional circulation,

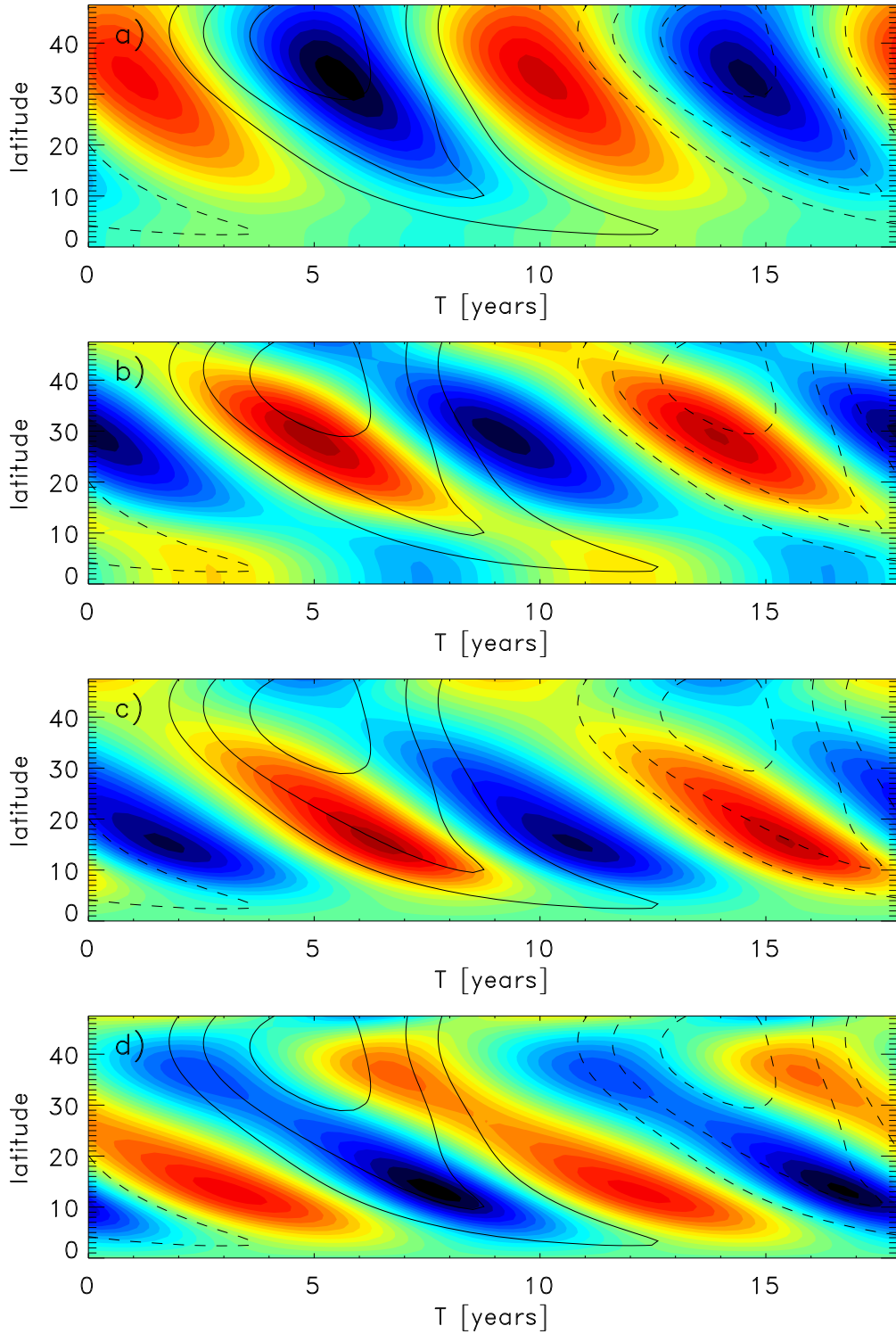


Figure 5. Model results. a) Surface temperature variation (blue: cold, red: hot, amplitude: 0.2 K). b) Torsional oscillations (blue slower, red faster rotation; amplitude: 1.35 nHz). c) Meridional flow variation at  $r = 0.985 R_{\odot}$  (blue: equatorward, red poleward motion; amplitude:  $2.3 \text{ m s}^{-1}$ ). d) Meridional flow variation at  $r = 0.93 R_{\odot}$  (blue: equatorward, red poleward motion; amplitude:  $0.22 \text{ m s}^{-1}$ ). The variation of the meridional flow pattern at  $r = 0.985 R_{\odot}$  is almost in anti-correlation to the flow at  $r = 0.93 R_{\odot}$  ( $\sim 50 \text{ Mm}$  depth). In all four panels the contour lines indicate the butterfly diagram computed from the toroidal field at the base of the convection zone.

as required for a flux-transport dynamo, follows self-consistently through the Coriolis force resulting from the differential rotation.

The computed differential rotation and meridional flow are used to advance the magnetic field in the flux-transport dynamo model, while the magnetic field is allowed to feed back through the meanfield Lorentz-force  $\langle \mathbf{J} \rangle \times \langle \mathbf{B} \rangle$ .

We find in our model that the Lorentz-force feedback can only account for the poleward propagating branch of the torsional oscillations, while the equatorward propagating branch in latitudes beneath  $30^\circ$  requires additional physics. Parameterizing the idea proposed by Spruit [15] that the low latitude torsional oscillation is a geostrophic flow caused by increased radiative loss in the active region belt (due to small scale magnetic flux) leads in our model to a surface oscillations pattern in good agreement with observations. In order to force a torsional oscillation with around 1 nHz amplitude a temperature variation of around 0.2 K is required. As a side effect the cooling produces close to the surface (in our model at  $r = 0.985 R_\odot$ ) an inflow into the active region belt of around  $2.3 \text{ m s}^{-1}$ .

Figure 5 summarizes the results of the model. Figure 5a shows the temperature fluctuation (color shades) caused by increased surface cooling in the active region belt. The contour lines indicate the magnetic butterfly diagram computed from the toroidal field at the base of the convection zone in the model. At the equatorward side of the active region belt (indicated by the butterfly diagram) the rotation rate is increased, which is consistent with the increased poleward meridional flow transporting material toward the axis of rotation. On the poleward side of the active region belt the rotation rate is lower, while the meridional flow perturbation is equatorward. At a depth of around 50 Mm (Fig. 5d) the meridional flow perturbation is almost anti-correlated to the surface flow (active region belt outflow), indicating that the surface cooling drives a flow system that closes in the upper third of the convection zone. The flow amplitude at a depth of 50 Mm is around one order of magnitude lower compared to the surface flow due to the significant increase in density.

### 3. CONCLUSION

The model reproduces the observations qualitatively, in particular the phase of the solar-cycle variations of the flows. Near the surface, the model is in remarkable agreement with the data: the torsional oscillation amplitude and the time-varying component of the meridional flow are predicted with the correct amplitude. Deeper in the interior, however, it appears that the model underestimates the amplitude of the time variations by an order of magnitude. Overall, it is fair to say that the model is encouraging.

The lower velocity seen in the dynamo model at depth is a consequence of mass conservation (strong increase

in density with depth). The much larger outflow which is observed in the data cannot be balanced by an inflow close to the surface unless it is confined to a very narrow layer. The observations may perhaps indicate that there is an upflow beneath the active region belt in the lower half of the convection zone, that turns into an outflow at around 60 Mm depth. It may be that a local treatment of the regions of strong magnetic field concentrations (sunspots and active regions) is necessary to obtain a better match between the model and the data. On the observational side, we are working toward a full inversion of the travel-time measurements to obtain improved and more reliable estimates of the depth variations of the flows.

### ACKNOWLEDGMENTS

The National Center for Atmospheric Research is sponsored by the National Science Foundation. M. Rempel thanks Prof. Schüssler and the Max-Planck-Institut für Sonnensystemforschung for their hospitality.

### REFERENCES

- [1] Duvall, T. L. & Gizon, L. 2000, *Solar Phys.*, 192, 177
- [2] Gizon, L., Duvall, T. L., & Schou, J. 2003, *Nature*, 421, 43
- [3] Zhao, J. & Kosovichev, A. G. 2003, in *Local and Global Helioseismology: The Present and Future*, ESA SP-517, 417
- [4] Komm, R. W., Howard, R. F., & Harvey, J. W. 1993a, *Solar Phys.*, 145, 1
- [5] Giles, P. M. 1999, Ph.D. Thesis, Stanford University
- [6] Beck, J. G., Gizon, L., & Duvall, T. L. 2002, *Astrophys. J.*, 575, L47
- [7] Howe, R., Komm, R., Hill, F., Ulrich, R., Haber, D. A., Hindman, B. W., Schou, J., Thompson, M. J. 2006, *Solar Phys.*, 235, 1
- [8] Zhao, J. & Kosovichev, A. G. 2004, *Astrophys. J.*, 603, 776
- [9] Chou, D.-Y. & Dai, D. 2001, *Astrophys. J.*, 559, L175
- [10] Rempel, M. 2005, *Astrophys. J.*, 622, 1320
- [11] Rempel, M. 2006, *Astrophys. J.*, 647, 662
- [12] Dikpati, M. & Charbonneau, P. 1999, *Astrophys. J.*, 518, 508
- [13] Dikpati, M. & Gilman, P. A. 2001, *Astrophys. J.*, 559, 428
- [14] Kitchatinov, L. L. & Rüdiger, G. 1993, *Astron. Astrophys.*, 276, 96
- [15] Spruit, H. C. 2003, *Solar Phys.*, 213, 1